The Journal of Chemical Physics

RESEARCH ARTICLE | OCTOBER 23 2020

Theoretical description of hyperpolarization formation in the SABRE-relay method

Stephan Knecht; Danila A. Barskiy ; Gerd Buntkowsky ; Konstantin L. Ivanov

J. Chem. Phys. 153, 164106 (2020)
https://doi.org/10.1063/5.0023308

The Journal of Chemical Physics ARTICLE scitation.org/journal/jcp

Theoretical description of hyperpolarization formation in the SABRE-relay method

Cite as: J. Chem. Phys. 153, 164106 (2020); doi: 10.1063/5.0023308
Submitted: 28 July 2020 • Accepted: 2 October 2020 •
Published Online: 23 October 2020

Stephan Knecht,[1] Danila A. Barskiy,[2] Gerd Buntkowsky,[1,a)] and Konstantin L. Ivanov[3,a)]

AFFILIATIONS

[1]Eduard-Zintl Institute for Inorganic and Physical Chemistry, TU Darmstadt, Darmstadt 64287, Germany
[2]University of California at Berkeley, College of Chemistry and QB3, Berkeley, California 94720, USA
[3]International Tomography Center, Siberian Branch of the Russian Academy of Sciences, and Novosibirsk State University, Novosibirsk 630090, Russia

[a)]**Authors to whom correspondence should be addressed:** gerd.buntkowsky@chemie.tu-darmstadt.de and ivanov@tomo.nsc.ru

ABSTRACT

SABRE (Signal Amplification By Reversible Exchange) has become a widely used method for hyper-polarizing nuclear spins, thereby enhancing their Nuclear Magnetic Resonance (NMR) signals by orders of magnitude. In SABRE experiments, the non-equilibrium spin order is transferred from parahydrogen to a substrate in a transient organometallic complex. The applicability of SABRE is expanded by the methodology of SABRE-relay in which polarization can be relayed to a second substrate either by direct chemical exchange of hyperpolarized nuclei or by polarization transfer between two substrates in a second organometallic complex. To understand the mechanism of the polarization transfer and study the transfer efficiency, we propose a theoretical approach to SABRE-relay, which can treat both spin dynamics and chemical kinetics as well as the interplay between them. The approach is based on a set of equations for the spin density matrices of the spin systems involved (i.e., SABRE substrates and complexes), which can be solved numerically. Using this method, we perform a detailed study of polarization formation and analyze in detail the dependence of the attainable polarization level on various chemical kinetic and spin dynamic parameters. We foresee the applications of the present approach for optimizing SABRE-relay experiments with the ultimate goal of achieving maximal NMR signal enhancements for substrates of interest.

I. INTRODUCTION

In less than a decade after its discovery,[1] the Signal Amplification By Reversible Exchange (SABRE) method[2,3] has evolved into an established tool for enhancing weak Nuclear Magnetic Resonance (NMR) signals of various nuclei, such as ^{1}H,[1–3] ^{13}C,[1,4–6] ^{15}N,[4,5,7–9] ^{19}F,[10,11] and ^{31}P.[12,13] Notably, SABRE can be used to boost the NMR signal of biologically important molecules such as antibiotics, vitamins,[14,15] and biorthogonal molecular tags.[16]

SABRE belongs to the family of Para-Hydrogen Induced Polarization (PHIP) methods, which have been developed in the pioneering works[17–20] of Weitekamp, Bowers, Bargon, and co-authors and since then become a widely used approach to NMR signal enhancement. In the SABRE method, strong non-equilibrium nuclear spin polarization of a suitable substrate, termed spin hyperpolarization, is generated. The source of this polarization is parahydrogen (pH$_2$), that is, the dihydrogen molecule in its nuclear spin singlet state. In SABRE experiments, the spin order of pH$_2$ is transferred to the substrate (S$_a$) in a transient complex (C$_1$), which simultaneously binds S$_a$ and pH$_2$. After dissociation of the complex, the generated hyperpolarization is accumulated in the free S$_a$ pool. The corresponding reaction scheme is shown in Fig. 1(a). A great advantage of the SABRE method compared to other hyperpolarization techniques is that the underlying chemical reactions are reversible and the polarization process can be repeated multiple times[21,22] by flushing fresh pH$_2$ through the solution. As far as the mechanism of the polarization process is concerned, it usually relies on coherent spin dynamics; chemical components taking part in this process are indicated by arrows [Fig. 1(a)]. Suitable conditions for polarization transfer are generated at low fields (hyperpolarization of protons)[1,23–25] or

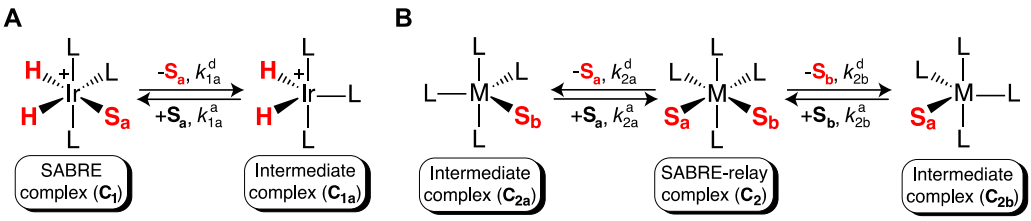

FIG. 1. Schematic representation of the SABRE-relay process involving two organometallic complexes. (a) Both the SABRE substrate (S_a) and parahydrogen (pH_2, not shown) in solution bind reversibly to a reaction intermediate (C_{1a}) to form the main SABRE complex C_1; substrate dissociation and association reaction rates are denoted as k^d_{1a} and k^a_{1a}, respectively. (b) Hyperpolarized SABRE substrate (S_a) is coordinated with another substrate (S_b), usually not amenable to direct SABRE, to a second organometallic complex C_2; dissociation and association rates are denoted as k^d_{2a} and k^a_{2a}, and k^d_{2b} and k^a_{2b} for exchange reactions involving S_a and S_b, respectively. In the second complex, polarization can be transferred from S_a to S_b via spin–spin couplings.

even under zero-to-ultralow-field conditions (namely, hyperpolarization of hetero-nuclei).[4,5,26–28] Alternatively, one can use NMR radiofrequency (RF) pulses for generating hyperpolarization at high magnetic fields.[22,29–36]

The range of substrates amenable to SABRE generated in the direct way (in the following, simply called SABRE) is limited to molecules that can bind reversibly to Ir-based organometallic complexes used as SABRE catalysts. Thus, SABRE substrates are usually heterocycles containing an electron-donating atom—typically, nitrogen—making it possible to hyperpolarize the derivatives of pyridine, purine, diazirines, Schiff bases, and others.[37] The class of molecules amenable to pH_2-based hyperpolarization via SABRE can be significantly extended by using a novel method termed SABRE-relay[38–43] [the reaction schemes are shown in Figs. 1(b) and 2] recently introduced by the group of Duckett. The method utilizes either chemical exchange[39] of hyperpolarized protons between the main SABRE-active substrate S_a and a second substrate S_b or transfer of hyperpolarization to S_b in a second complex (C_2),[38] which simultaneously binds S_a to S_b and, thus, couples both their spin systems by intramolecular spin–spin couplings (J-couplings) in C_2. The SABRE-relay approach allows one to polarize substrates, which are otherwise not amenable to SABRE polarization[39] using Ir-based complexes (which bind only special classes of molecules).

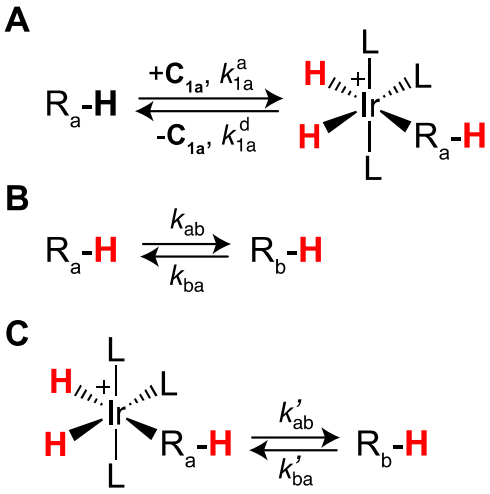

FIG. 2. Schematic representation of the SABRE-relay process involving hydrogen exchange between two substrates (typical for amines). (a) Primary SABRE-hyperpolarization process of R_a–H. (b) Labile protons of the free substrate R_a–H (S_a) undergo chemical exchange with protons of the free substrate R_b–H (S_b), which becomes hyperpolarized in the course of the exchange process. (c) Direct proton exchange is taking place between complex-bound substrate R_a–H (S_a) and free substrate R_b–H (S_b).

In order to fully exploit the broad application potential of the SABRE-relay, we develop a consistent theoretical description of the polarization formation. The theoretical approach used in this work employs the density-matrix formalism,[44] previously utilized to simulate SABRE polarization formation.[45,46] Our theory explicitly treats the spin dynamics in the SABRE complex, the substrates, and their interplay via chemical exchange. Here, we limit ourselves to coherent polarization transfer at a suitable low external magnetic field, i.e., we do not consider the situation of polarization formation by incoherent polarization processes[47,48] or high-field RF pulse sequences, since this would require the consideration of the time-dependent spin Hamiltonians of S_1, S_2, C_1, and C_2. Such a generalization of the theory is possible,[45] but it is beyond the scope of this work. The developed theoretical model is used for the analysis of the polarization formation process by investigating the factors affecting the resulting polarization, thus enabling the optimization of NMR signal enhancement in the SABRE-relay process.

II. CHEMICAL KINETIC SCHEMES

We start with a simpler approach to the problem, utilizing chemical kinetics schemes. First, we outline the derivation of the general chemical kinetics scheme[49] of the SABRE process. Subsequently, we introduce the kinetic equations of the SABRE-relay process.

A. Chemical kinetic scheme of SABRE

Here, we describe a SABRE kinetics approach, which is the first step for introducing a density matrix treatment of SABRE-relay. The consideration in this section is based on the treatment introduced by some of us previously[49] and closely follows the original formulation. In Fig. 1, we depict the proposed SABRE kinetic scheme, though in a simplified form. Hereafter, all concentrations are written in square brackets, i.e., [X] stands for the concentration of the compound X.

As a starting point, we write down the differential kinetic equations that arise from the exchange processes depicted in Fig. 1(a),

$$C_1 \leftrightarrows S_a + C_{1a}. \tag{1}$$

The association of substrate S_a as depicted in Fig. 1(a) and Eq. (1) describes a second-order reaction. If the concentration $[C_{1a}]$ of the intermediate C_{1a} stays constant, this reaction proceeds with an effective pseudo-first-order rate constant $k^a_{1a} = k^a_{Sa}[C_{1a}]$. Additionally, here, we do not explicitly describe the exchange of free hydrogen in solution with the intermediate SABRE complex C_{1a} but rather assume that it is fast on NMR time scales, and thus, the spin state of the protons in C_{1a} is taken the same as that of the protons in the pool of dissolved H_2 molecules. A treatment of the reaction intermediates is possible[36] but beyond what is required for the presented work. With these assumptions, it is possible to write down the differential equations for the concentrations of the free substrate and the main SABRE complex arising from the exchange process of Eq. (1),

$$\frac{d[C_1]}{dt} = k^a_{1a}[S_a] - k^d_{1a}[C_1], \tag{2a}$$

$$\frac{d[S_a]}{dt} = -k^a_{1a}[S_a] + k^d_{1a}[C_1]. \tag{2b}$$

The superscript indices "a" and "d" in Eq. (2) refer to the association or dissociation rate constants for the complex C_1, respectsively. These equations are the starting points of the SABRE-relay exchange schemes described below.

B. Chemical kinetic scheme of SABRE-relay

In the next step, chemical exchange of hyperpolarized protons is to be considered (see Fig. 2). Consequently, we amend the above kinetics equations by introducing the exchange reaction of the SABRE substrate S_a with a second, SABRE inactive, substrate molecule S_b in solution,

$$S_a \leftrightarrows S_b,$$

and writing down a modified differential equation for $[S_a]$ and a new equation for $[S_b]$,

$$\frac{d[S_a]}{dt} = -k^a_{1a}[S_a] + k^d_{1a}[C_1] - k_{ab}[S_a] + k_{ba}[S_b],$$

$$\frac{d[S_b]}{dt} = k_{ab}[S_a] - k_{ba}[S_b].$$

Here, k_{ab} and k_{ba} are reaction rates (hereafter given in s^{-1}) for chemical exchange of hyperpolarized nuclear spins (e.g., protons) between two substrates. These equations are similar to Eq. (2a) but now contain additional terms, which stand for chemical exchange between S_a and S_b. As usual, when the system is in chemical equilibrium, there is a straightforward relation between the exchange rates and the concentrations,

$$\frac{[S_a]}{[S_b]} = \frac{k_{ba}}{k_{ab}}.$$

It should be noted that we assume a simple first-order exchange of protons between the two substrate pools. This assumption might not always hold true but can be accounted for by introducing concentration-dependent exchange rates k_{ab} and k_{ba}.

Next, we treat a more complex situation, where a second organometallic complex C_2 is involved in the SABRE-relay process.[38] Such a complex binds both S_a and S_b [see Fig. 1(b)]; in the following, we extend the reaction scheme by considering the coordination of S_a and S_b with this new complex C_2. To do so, we assume that the coordination of substrate ligands to C_2 proceeds in a manner similar to the case of the main SABRE complex. Specifically, we assume that C_2 dissociates into one of two reaction intermediates, C_{2a} or C_{2b}, by dissociating S_a or S_b, respectively. Under these conditions, we arrive at the reaction scheme given in Eq. (3) and depicted in Fig. 1(b),

$$\begin{aligned} S_a + C_{2a} &\leftrightarrows C_2, \\ S_b + C_{2b} &\leftrightarrows C_2. \end{aligned} \tag{3}$$

As has been done in Subsection II A, we define the effective association rates k^a_{2a} and k^a_{2b} for S_a and S_b with their respective intermediate complexes C_{2a} and C_{2b} as

$$k^a_{2a} = k^a_{Sa}[C_{2a}], \quad k^a_{2b} = k^a_{Sb}[C_{2b}].$$

As a simplifying assumption, in Eq. (3), we consider only complexes binding both S_a and S_b and do not describe complexes binding solely S_a or S_b. Furthermore, we assume that any intermediates in this process are too short-lived to substantially alter the coherent spin dynamics in the system. The exchange process of Fig. 1(b) obeys the following kinetic equations:

$$\frac{d[S_a]}{dt} = -\left(k^a_{1a} + k^a_{2a}\right)[S_a] + k^d_{1a}[C_1] + k^d_{2a}[C_2],$$

$$\frac{d[S_b]}{dt} = -k^a_{2b}[S_b] + k^d_{2b}[C_2],$$

$$\frac{d[C_2]}{dt} = k^a_{2a}[S_a] + k^a_{2b}[S_b] - \left(k^d_{2a} + k^d_{2b}\right)[C_2].$$

In Sec. III, we introduce the equations for the density matrices of the substrates and complexes involved. Such equations describe both the spin dynamics and chemical kinetics, as well as their interplay.

III. DENSITY MATRIX CALCULATIONS

Here, we generalize the density matrix approach, which has been previously used to describe the SABRE process, to the more complex situation of SABRE-relay. Specifically, we introduce the density-matrix equations for the species S_b to which hyperpolarization is relayed, and, if needed, for the SABRE-relay complex C_2. The density matrix operations, which are used to describe association and dissociation (direct product and partial trace), are the same as those used before[46] and are explained in more detail in Subsection III C.

A. SABRE-relay via chemical exchange

In the case of SABRE-relay via chemical exchange, it becomes necessary to introduce the density matrix for the species S_b and consider chemical exchange between S_a and S_b. Here, we use a simplified spin system, namely, we assume that the molecules of species S_a and S_b contain only a single proton, which is exchanging with the forward and backward rates k_{ab} and k_{ba}, respectively [Fig. 2(a)]. The main SABRE complex C_1 is modeled here as a three-spin system consisting of two nuclei originating from pH_2 and the complex-bound substrate S_a. Thus, the set of equations for the three density matrices of interest (density matrices of the two substrates, $\hat{\sigma}_{S_a}$ and $\hat{\sigma}_{S_b}$ and complex $\hat{\sigma}_{C_1}$) is as follows:

$$\begin{aligned}
\frac{d}{dt}\hat{\sigma}_{S_a} &= \hat{\hat{L}}_{S_a}\hat{\sigma}_{S_a} + k_{1a}^{d}\mathrm{Tr}_{C_{1a}}\{\hat{\sigma}_{C_1}\} - k_{1a}^{a}\hat{\sigma}_{S_a} + k_{ba}\hat{\sigma}_{S_b} - k_{ab}\hat{\sigma}_{S_a},\\
\frac{d}{dt}\hat{\sigma}_{C_1} &= \hat{\hat{L}}_{C_1}\hat{\sigma}_{C_1} - k_{1a}^{d}\hat{\sigma}_{C_1} + k_{1a}^{a}\{\hat{\rho}_{H_2}\otimes\hat{\sigma}_{S_a}\},\\
\frac{d}{dt}\hat{\sigma}_{S_b} &= \hat{\hat{L}}_{S_b}\hat{\sigma}_{S_b} - k_{ba}\hat{\sigma}_{S_b} + k_{ab}\hat{\sigma}_{S_a}.
\end{aligned} \tag{4}$$

The system of differential equations (4) describes the exchange of protons between the species S_a and S_b only when they both are in the free form. Here, $\hat{\hat{L}}_X = -i\hat{\hat{H}}_X + \hat{\hat{R}}_X$ is the Liouville operator of the species X, where $\hat{\hat{H}}$ is the commutator-defined superoperator of the spin Hamiltonian, $\hat{\hat{H}}_X\hat{\sigma}_X = [\hat{H}_X, \hat{\sigma}_X]$, and $\hat{\hat{R}}_X$ is the relaxation superoperator. Association and dissociation of complexes as is mathematically treated by the direct product (denoted by symbol $\otimes$) and partial trace operation $\mathrm{Tr}_x\{y\}$ are described in more detail in the next paragraph. The precise form of the Hamiltonians $\hat{H}_X$ is specified in Subsection III C; we always assume that the conditions for efficient coherent polarization transfer with respect to the magnetic field are achieved, meaning that the system is under the proper Level Anti-Crossing (LAC) conditions.[24,25]

Simple arguments on the way of writing density matrix equations (4) are the following. As a starting point, we use the corresponding kinetic equations for the concentrations and replace $[X] \to \hat{\sigma}_X$ in all equations, i.e., replace the concentration by the corresponding density matrix, which is normalized as $\mathrm{Tr}\{\hat{\sigma}_X\} = [X]$. There are only two additional issues, which have to be taken into account: (i) terms describing the nuclear spin evolution $\hat{\hat{L}}_X\hat{\sigma}_X$ should be added and (ii) the dimensionality of the matrices on the left-hand side and on the right-hand side should be matched. To do so, when necessary, we reduce dimensionality by the partial trace operation (when the substrate is dissociated from the complex) and increase dimensionality by taking the direct product, $\otimes$, of density matrices (when the substrate and the complex are associated). These simple considerations are in agreement with the rigorous derivation of kinetic equations, which can be found elsewhere.[50,51]

In the particular case under consideration, Eq. (4), the terms describing substrate exchange with the complex are introduced in the same way as in Ref. 46. To reduce the dimensionality of the term describing dissociation in the equation for $\hat{\sigma}_{S_a}$, we take the partial trace over the spin states of hydrides in the complex C_1. To increase the dimensionality of the density matrix in the term, which describes association in the equation for $\hat{\sigma}_{C_1}$, we take the direct product of $\hat{\sigma}_{C_{1a}} = \hat{\rho}_{H_2}$ and $\hat{\sigma}_{S_a}$, where $\hat{\rho}_{H_2} = |S\rangle\langle S|$ is the normalized spin density matrix of H_2. It is given by the projection operator onto the singlet state $|S\rangle$ (in contrast to $\hat{\sigma}_X$ matrices, the trace of the density matrix $\hat{\rho}_{H_2}$ is equal to unity). The terms describing proton exchange are introduced by using the rate constants k_{ab} and k_{ba}.

We would like to emphasize that an important assumption of Eq. (4) is that the spin state of the intermediate C_{1a} is represented by the state of pH_2 in solution. Hence, we neglect any competition between hydrogen and substrate binding in the formation of the main SABRE complex as well as any coherent or incoherent spin evolution in the intermediates. Such effects could be included by adding an explicit density matrix equation for the intermediate C_{1a}, as has been done before.[52]

So far, we only considered the situation where the protons of S_a and S_b exchange, assuming that both substrates are in their free form in solution, i.e., when S_a is not bound to the SABRE complex C_1. However, the situation may arise, where the protons of the catalyst-bound species S_a exchange with those of S_b [see Fig. 2(c)]. Indeed, chemical exchange involving complex-bound substrates in SABRE has been reported before in the case of coordinated water.[53,54]

We can account for this process, by adding the appropriate terms to Eq. (4),

$$\begin{aligned}
\frac{d}{dt}\hat{\sigma}_{S_a} &= \hat{\hat{L}}_{S_a}\hat{\sigma}_{S_a} + k_{1a}^{d}\mathrm{Tr}_{C_{1a}}\{\hat{\sigma}_{C_1}\} - k_{1a}^{a}\hat{\sigma}_{S_a} + k_{ba}\hat{\sigma}_{S_b} - k_{ab}\hat{\sigma}_{S_a},\\
\frac{d}{dt}\hat{\sigma}_{C_1} &= \hat{\hat{L}}_{C_1}\hat{\sigma}_{C_1} - k_{1a}^{d}\hat{\sigma}_{C_1} + k_{1a}^{a}\{\hat{\rho}_{H_2}\otimes\hat{\sigma}_{S_a}\}\\
&\quad - k'_{ab}\hat{\sigma}_{C_1} + k'_{ba}\{\mathrm{Tr}_{S_a}\{\hat{\sigma}_{C_1}\}\otimes\hat{\sigma}_{S_b}\},\\
\frac{d}{dt}\hat{\sigma}_{S_b} &= \hat{\hat{L}}_{S_b}\hat{\sigma}_{S_b} - (k_{ba}+k'_{ba})\hat{\sigma}_{S_b} + k_{ab}\hat{\sigma}_{S_a} + k'_{ab}\mathrm{Tr}_{C_{1a}}\{\hat{\sigma}_{C_1}\}.
\end{aligned} \tag{5}$$

For simplicity, we assume here that this process also occurs with the first-order rate constants k'_{ab} for forward and k'_{ba} for reverse exchange. We again assume that any other reaction intermediates are too short-lived to alter the spin dynamics.

We would like to point out that the present study is focused solely on a three-spin system for the main SABRE complex and a single exchanging nucleus for the SABRE-relay process. This is the minimal system allowing one to reproduce the main features of SABRE formation.[24,25] Previous works have shown that the presence of additional spin-1/2 nuclei can alter the spin dynamics of the system[5] and their inclusion may become necessary in future studies. Such an extension of the theory is straightforward in the density matrix formalism, but it is computationally demanding. Furthermore, in real systems, the exchange dynamics are very likely influenced by additional exchanging sites in the molecule: such effects can be described by adding more chemical species and additional kinetic equations to system (5). Such extensions of the theory are beyond the scope of this work.

B. SABRE-relay in a second complex

Next, we formulate the set of equations suitable to describe the relayed transfer of polarization in a second SABRE-relay complex (see Fig. 3). Such a complex is treated in a similar way as the main SABRE complex, in the sense that it temporarily binds both S_a and S_b. While both substrates reside at the catalyst, the spins of both S_a and S_b are connected by scalar spin–spin couplings, J-couplings,

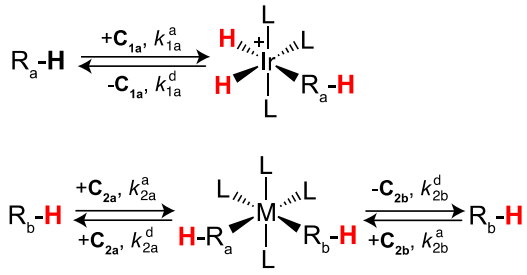

FIG. 3. Schematic representation of the SABRE-relay process involving chemical exchange between two organometallic complexes. Note that polarization transfer to protons is shown, while other nuclei in the second complex can be polarized as well under optimal magnetic field conditions.

allowing for coherent transfer of spin order. The system of equations used in this work is written as follows:

$$\begin{aligned}
\frac{d}{dt}\hat{\sigma}_{S_a} &= \hat{\hat{L}}_{S_a}\hat{\sigma}_{S_a} + k^{d}_{1a}\mathrm{Tr}_{C_{1a}}\{\hat{\sigma}_{C_1}\} - (k^{a}_{1a} + k^{a}_{2a})\hat{\sigma}_{S_a} + k^{d}_{2a}\mathrm{Tr}_{S_b}\{\hat{\sigma}_{C_2}\},\\
\frac{d}{dt}\hat{\sigma}_{C_1} &= \hat{\hat{L}}_{C_1}\hat{\sigma}_{C_1} - k^{d}_{1a}\hat{\sigma}_{C_1} + k^{a}_{1a}\{\hat{\rho}_{H_2}\otimes\hat{\sigma}_{S_a}\},\\
\frac{d}{dt}\hat{\sigma}_{S_b} &= \hat{\hat{L}}_{S_b}\hat{\sigma}_{b} + k^{d}_{2b}\mathrm{Tr}_{S_a}\{\hat{\sigma}_{C_2}\} - k^{a}_{2b}\hat{\sigma}_{S_b},\\
\frac{d}{dt}\hat{\sigma}_{C_2} &= \hat{\hat{L}}_{C_2}\hat{\sigma}_{C_2} - \left(k^{d}_{2a} + k^{d}_{2b}\right)\hat{\sigma}_{C_2} + k^{a}_{2a}\{\hat{\sigma}_{S_a}\otimes\mathrm{Tr}_{S_a}\{\hat{\sigma}_{C_2}\}\}\\
&\quad + k^{a}_{2b}\{\mathrm{Tr}_{S_b}\{\hat{\sigma}_{C_2}\}\otimes\hat{\sigma}_{b}\}.
\end{aligned} \tag{6}$$

Here, we treat the spin dynamics for all chemical species involved, i.e., substrates S_a and S_b and complexes C_1 and C_2. As previously, we introduce the spin evolution of each species by using the corresponding Liouville operator; chemical exchange is introduced in the same way as above (when necessary, the dimensionality of the density matrices is reduced by taking partial trace or increased by taking the direct product as described in Subsection III C).

C. Implementation of the model

Using sets of Eqs. (4) and (6), one can treat the reaction and spin dynamics for both schemes of the SABRE-relay experiment. However, we still need to comment on implementation of the model, explaining how different superoperators should be introduced in the numerical scheme and how the set of equations should be solved. We also comment on the NMR observables discussed in the rest of this paper.

In contrast to the density matrix formulations previously used to describe SABRE,[46] the above systems of equations are non-linear, which precludes using a simple linear propagation operator to solve them. Here, we chose to either integrate the system numerically (typical time traces can be found in Appendix A) using the Runge–Kutta method or obtain the steady-state solution by solving the equation systems using the Levenberg–Marquardt method. When integration was used, the system was evolved to a time point of at least five times the T_1-relaxation time of the slowest relaxing spin species in order to guarantee that a steady-state of the hyperpolarization built-up has been reached. All calculations were performed on a standard office laptop with two cores running MATLAB 2019a (Mathworks, USA). Numerical integration was carried out using MATLAB's ode45 or ode113 functions, and each integration of the system took between 1 s and 30 s. When solving the equation system to obtain the steady-state solution using the Levenberg–Marquardt method implemented in MATLAB's "fsolve" functionality, the calculation time was approximately an order of magnitude shorter than for direct integration. We assume that initially all spins in the system are non-polarized, except for the pH_2-nascent protons.

The spin dynamics are governed by the Liouville operators of the individual species introduced in Eq. (6),

$$\hat{\hat{L}}_X = -i\hat{\hat{H}}_X + \hat{\hat{R}}_X. \tag{7}$$

Here, the spin Hamiltonians of each species, comprising N spins, are written as follows:

$$\hat{\mathcal{H}} = \sum_{i=1}^{N}\omega_i\hat{I}_{i,z} + \sum_{i<j}2\pi J_{ij}\left(\hat{\boldsymbol{I}}_1\cdot\hat{\boldsymbol{I}}_2\right). \tag{8}$$

Here, $\omega_i = -\gamma B_z(1+\delta_i)$, where γ_i and δ_i are the gyromagnetic ratio and chemical shift of the ith spin, respectively, B_z is the strength of the external magnetic field parallel to the z-axis, J_{ij} is the scalar coupling of the respective spins. In the case of numerical integration and dealing with only one spin species (namely, protons), we neglect the large Larmor frequency in order to speed up calculations and just retain the chemical shift part of the Zeeman term taking $\omega_i = -\gamma_H B_z\delta_i$. When the steady state solution was obtained or X-nuclei were considered, the full Zeeman term was retained. To model relaxation, we employ a previously described treatment of random fluctuating fields.[55] The parameters used (unless otherwise stated in Sec. IV) can be found in Table I. Considering spin relaxation, we always use a homogeneous term $\hat{\hat{R}}_X\hat{\sigma}_X$ rather than $\hat{\hat{R}}_X\left(\hat{\sigma}_X - \hat{\sigma}^{eq}_X\right)$, thus neglecting the small equilibrium spin polarization described by the density matrix $\hat{\sigma}^{eq}_X$. A more precise and elaborate approach would require correcting the elements of $\hat{\hat{R}}_X$ by Boltzmann factors for the spin transitions, as discussed, e.g., in a recent work by Bengs and Levitt.[56] However, in the case of (i) high-temperature (hence, very small Boltzmann factors for all spin transitions) and (ii) high polarization as compared to the tiny thermal polarization, these complexities are not required.

We assume all species to be in stationary conditions; thus, the association rates in Eq. (6) can be expressed in terms of the dissociation rate and the concentrations of the species in the system. More precisely, if we consider exchange between two species A and B with concentrations [A] and [B] as well as forward and reverse rates $k_{A\to B}$ and $k_{B\to A}$, we always check that the relation $\frac{k_{A\to B}}{k_{B\to A}} = \frac{[B]}{[A]}$ is fulfilled. This is needed to make sure that the trace of the individual density matrices and, hence, the concentrations in the system do not change during the calculations. In Appendix B, we briefly reiterate the density matrix treatment used to calculate the effects of exchange here. The parameters governing the spin-dynamics, i.e., J-couplings and chemical shifts, as well as the exchange rates of different species are also listed in Appendix B. We would like to stress that these parameters do not correspond to any specific system used in SABRE-relay. The reason for this is twofold: first, none of the SABRE-relay systems

is completely characterized, e.g., in terms of the relevant exchange rates; second, we do not have in hand a comprehensive dataset available for direct comparison with the theory. At the same time, the chosen parameters are well within the range, one should expect for such chemical systems.

For interpretation of the simulation results reported below, we calculate the polarization of the spins in different species in the following way:[46]

$$P(\mathrm{X}) = 2 \cdot \frac{\mathrm{Tr}\{\hat{\sigma}_{\mathrm{X}} \cdot \hat{I}_z\}}{\mathrm{Tr}\{\hat{\sigma}_{\mathrm{X}}\}}. \tag{9}$$

Additionally, in some cases, we are interested to calculate the NMR signal, which is proportional to magnetization, the product of spin polarization, and the concentration of the corresponding species X,

$$M_{\mathrm{eff}}(\mathrm{X}) = P(\mathrm{X}) \cdot [\mathrm{X}]. \tag{10}$$

IV. RESULTS AND DISCUSSION

A. SABRE-relay via chemical exchange

First, we examine the polarization levels for the second species S_b considering the SABRE-relay model of chemical exchange $S_a \leftrightarrows S_b$ [see Figs. 2(a) and 2(b)], as described by the set of Eq. (4). When both the main SABRE substrate S_a and the second substrate S_b undergo chemical exchange, which is sufficiently fast for equal redistribution of hyperpolarized nuclei between both pools, the polarization of both will decrease as the concentration of either one is increased [see Fig. 4(a), top]. Such a behavior has been previously predicted for the concentration dependence of the main SABRE substrate[46,49] and can be explained by the fact that only a limited amount of the substrate can be polarized by the main SABRE complex per unit time. On the other hand, the relaxation of the free substrate pool drives its polarization back to the small equilibrium value. Thus, at a certain concentration, the overall number of hyperpolarized spins will be the same, regardless of the size of the free substrate pools. Consequently, the average polarization decreases as the pool is increased. This effect can be better understood considering what happens to the effective magnetization (see Sec. III C) in the system, which is shown in Figs. 2(a) and 2(b). When the concentration of species S_b is low, so is its signal. As the concentration of S_b increases (we assume that S_b undergoes rapid exchange with species S_a), more and more of the hyperpolarized spins will be found in the S_b pool, rather than in the S_a pool. Consequently, the signal of S_b will increase and eventually plateau, while the signal of S_a decreases [see Fig. 4(a), bottom]. However, a distinction to the previously obtained results for the concentration dependence of SABRE polarization should be made: in the SABRE approach, the substrate molecules reduce the hyperpolarization efficiency by competing with pH_2 (the source of hyperpolarization) in the exchange with the main SABRE complex.

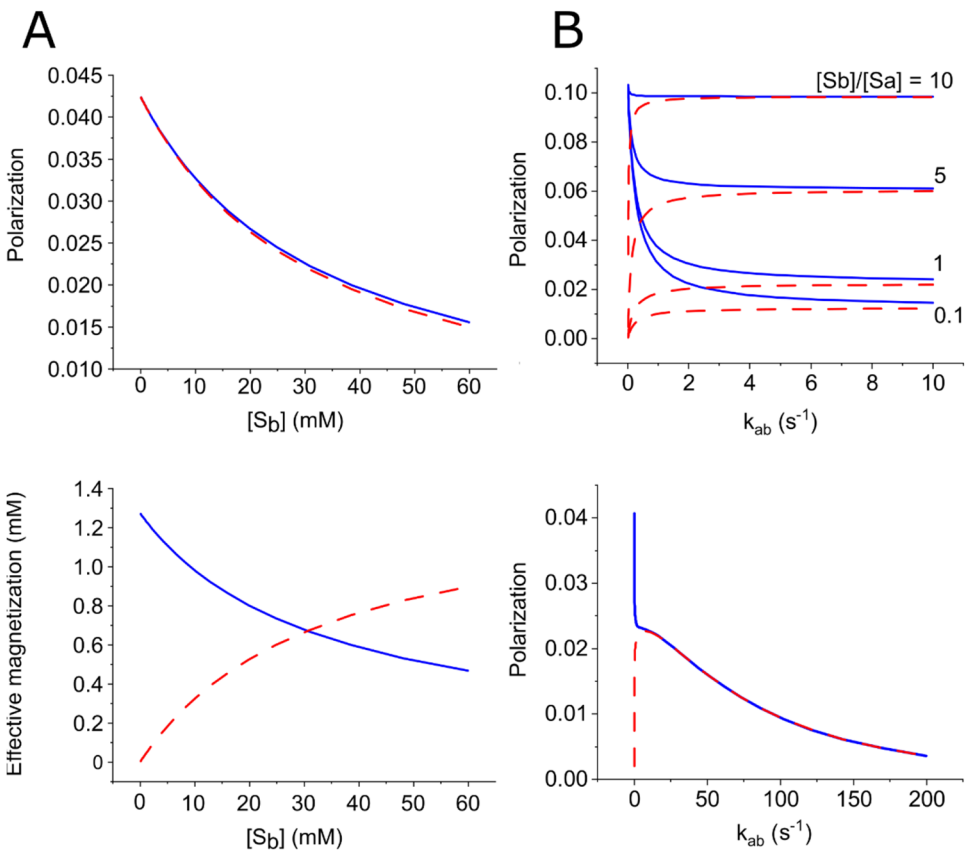

FIG. 4. (a) Polarization (top) and effective magnetization (bottom) of the main SABRE substrate (S_a, blue line) and the SABRE-relay substrate (S_b, red dashed line) as a function of the concentration [S_b], while [S_a] = 30 mM is kept constant. (b) Top: polarization of the main SABRE substrate (S_a, blue line) and the SABRE-relay substrate (S_b, red dashed line) as a function of the exchange rate k_{ab} for different ratios [S_b]/[S_a]. Here, [S_a] = 10 mM is kept constant. Bottom: polarization of the main SABRE substrate (S_a, blue line) and the SABRE-relay substrate (S_b, red dashed line) depending on the exchange rate k_{ab} when free S_a and free S_b are exchanging (where [S_a] = [S_b] = 30 mM). Here, we account for both processes depicted in Figs. 2(b) and 2(c) with kinetic rate constants $k'_{ab} = k_{ab}$. Note that the process depicted in Fig. 2(c) interferes with the coherent polarization process of S_a in C_1 at high values of k'_{ab}.

Such a behavior is not occurring here for S_b, as the S_b molecules never bind to any complex.

Next, we want to explore the polarization dependence on the exchange rate of protons between S_a and S_b, which is plotted in Fig. 4(b), top. One can see that at low exchange rates, the second substrate is not polarized at all, while with an increasing rate of exchange, the polarization is distributed between both species S_a and S_b. The total polarization in this case depends on the relative concentrations (i.e., a larger pool of substrate again leads to a lower polarization value).

So far, exchange only between the two substrates in their free form was considered. If, however, the SABRE-relay substrate S_b is also exchanging (here, we assume that for simplicity, the rates are the same as for the free form) with the bound form of S_a in the main SABRE complex, as depicted in Fig. 2(c), the spin evolution changes significantly. In such a situation, the exchange between the protons of the two substrates interferes destructively with the coherent polarization transfer mechanism in the main SABRE complex. This is because a certain residence time at the catalyst is needed for effective coherent transfer of polarization from pH_2 to the substrate protons of S_a.[23,46,49] Consequently, when the proton exchange rates are too high, the efficiency of SABRE-relay drops significantly [see Fig. 4(b), bottom]. We speculate that this behavior might be the reason for the lower efficiency of the relayed SABRE polarization of amines reported in the presence of water in the sample.[41]

B. SABRE-relay in a second complex

Let us now turn to the situation where polarization is relayed in a second organometallic complex.

1. Polarization transfer mechanism

As mentioned before, in the scheme with two complexes, the transfer is not mediated by chemical exchange of protons, but by coherent transfer of polarization via J-couplings in the second complex (although chemical exchange of protons between ligands bound to the catalyst, as reported before,[53,54] could also be treated with the above equations in a straightforward way). The efficiency of spin polarization transfer between the two nuclei belonging to S_a and S_b will thus depend on the difference $\Delta\nu = \gamma_H B_z \Delta_\delta / 2\pi$ in their Zeeman interactions with the field frequency difference and J-couplings (here, Δ_δ is the chemical shift difference). Figure 5 shows the field dependence for a system of two indirectly coupled protons in the SABRE-relay complex. It should be noted that because of this small polarization field, already relatively small couplings can be efficient to transfer polarization between protons, even if their chemical shift difference is large (here, 10 ppm were assumed, which at 5 mT, corresponds to a frequency difference of ~2.5 Hz). However, for transfer to most X-nuclei, this process will become efficient only at the appropriate ultralow field, where SABRE polarization of protons is then again inefficient.[4] Hence, we see that the magnetic field strength, favorable for spin order transfer $pH_2 \rightarrow S_a$, is also suitable for the relayed polarization transfer $S_a \rightarrow S_b$ in the second complex when protons are considered.

2. Concentration dependences of polarization

When examining the predicted polarization dependence of the two substrates S_a and S_b on the concentration of the main SABRE complex C_1 as well as of the SABRE-relay complex C_2, a curious dependence is found. While an increase of C_1 leads to an increasing polarization of both substrates, eventually reaching a maximum, increase in the concentration of the SABRE-relay complex gives rise to a different behavior [see Fig. 6(a)]. At small $[C_2]$, the increase in the concentration of the SABRE-relay complex leads to an increase in the polarization of the SABRE-relay substrate, while at the same time, the polarization of the main SABRE substrate decreases. Upon further increase, however, S_a and S_b both decrease. This behavior is explained by the relatively fast relaxation ($R = 1\ s^{-1}$) of the substrates bound to the organometallic SABRE complexes, as assumed here. Thus, when the concentration of these complexes is increased, the effective T_1-relaxation time of the substrates, and consequently, their polarization, is reduced. However, for the main SABRE complex C_1, this reduction (caused by enhanced T_1-relaxation) is compensated by an increased production of hyperpolarized species in the system.

The dependence of hyperpolarization of the free substrates S_a and S_b on their concentrations, shown in Fig. 6(b), can be rationalized in the following way. When the $[S_a]$ concentration is increased, its polarization drops, similar to the results in Subsection IV A and as predicted by the previously formulated SABRE models.[46,49] Consequently, because S_a acts as the source of polarization distributed into the second complex, the polarization of S_b also decreases. When the concentration of S_b is varied, the behavior is somewhat different. Upon increase in $[S_b]$, its hyperpolarization decreases, reflecting the fact that the number of hyperpolarized molecules per unit of time, at best, is independent of the free substrate pool and its increase will not increase the hyperpolarized magnetization generated in the system. The polarization of S_a will reach a constant value, which is independent of the amount of SABRE-relay complexes in the system, because at high concentrations of S_b, the amount of molecules hyperpolarized by relayed transfer from S_a will stay constant (as now the SABRE-relay complex and not the concentration of S_b is the limiting factor).

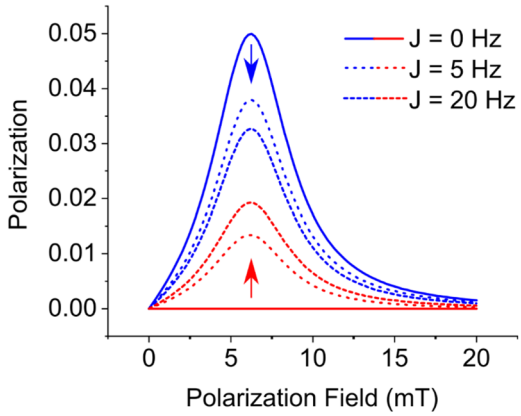

FIG. 5. Polarization field dependence of the main SABRE substrate (S_a, blue) and the SABRE-relay substrate (S_b, red) depending on the J-couplings in the SABRE-relay. Here, a chemical shift difference of 10 ppm between S_a and S_b was assumed.

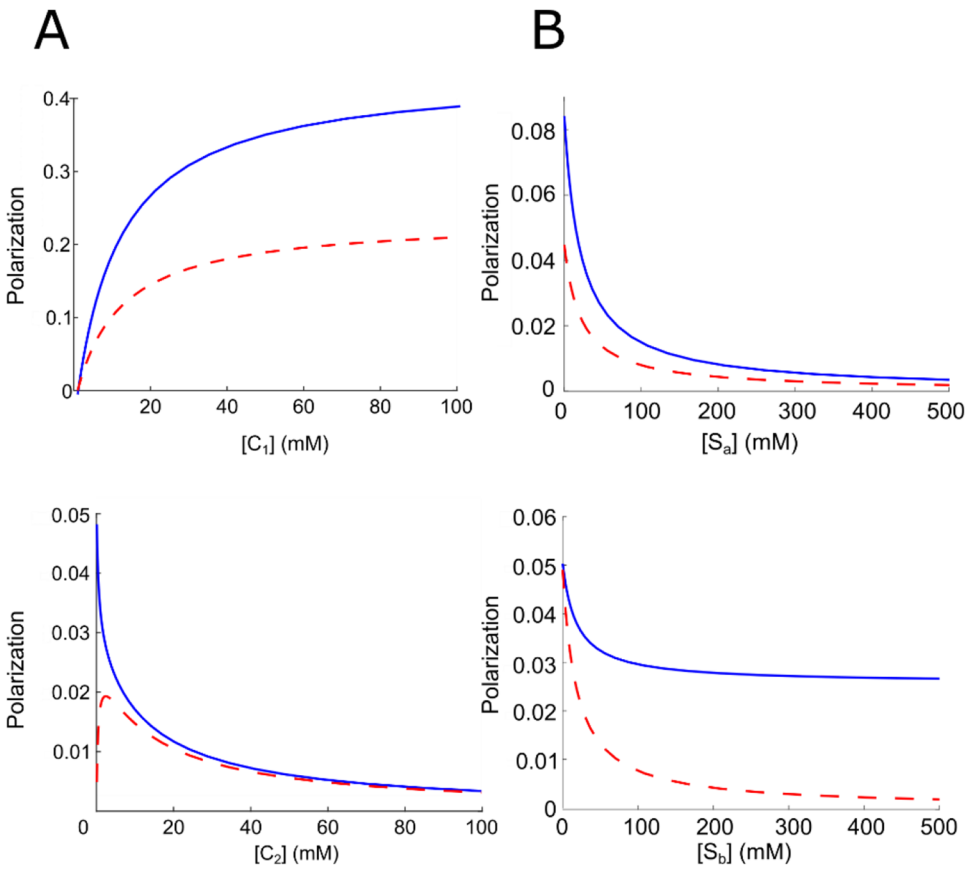

FIG. 6. (a) Polarization as a function of the concentration of the main SABRE complex C_1 (top) and SABRE-relay complex C_2 (bottom). Here, the results are shown for substrate S_a (blue line) and substrate S_b (red dashed line). While an increase in the $[C_1]$ concentration leads to an increase and eventual leveling-off of the polarization of both substrates, an increase in $[C_2]$ leads to a monotonous decrease in the polarization of S_1 and a dependence with a maximum for the polarization of S_b. (b) Polarization dependence of the main SABRE substrate (S_a, blue line) and the relay substrate (S_b, red dashed line) on the concentrations of the free substrate S_a (top) and S_b (bottom).

3. Dependence of polarization on exchange rate

We examined the dependence of the hyperpolarization generated by SABRE-relay not only on concentrations but also on the kinetic parameters, namely, on the exchange rates in complex C_2. For the coherent polarization transfer mechanism considered here, our investigation predicts an optimal dissociation rate in the second complex [see Fig. 7(a)]. This behavior is similar to that predicted[23,46] for SABRE, namely, at high exchange rates (and consequently, short lifetimes of the complex), the coherent transfer of polarization is suppressed, whereas at low exchange rates, the generated polarization is limited by relaxation.

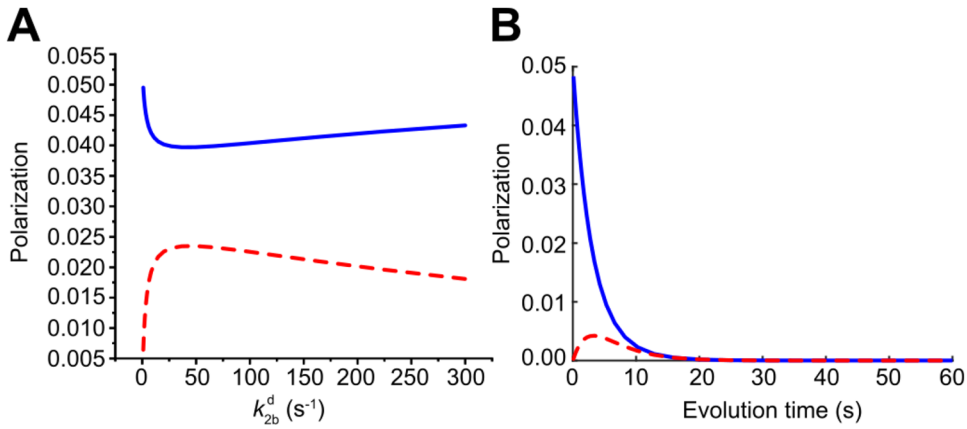

FIG. 7. (a) Polarization of the main SABRE substrate S_a (blue line) and the relay substrate S_b (red dashed line) as a function of the dissociation rate (k^d_{2b}) of the SABRE-relay complex. (b) Temporal evolution of polarization (ensemble-averaged quantity) of the proton of the main SABRE substrate S_a (blue line) and a ^{31}P nucleus in the second complex C_2 (red dashed line). In the calculation, we assumed the initial polarization of protons at the optimal SABRE field, 6 mT with a subsequent evolution at an ultralow field, here, at 1 μT.

4. Relayed transfer of polarization to heteronuclei

As discussed above, the relayed polarization transfer can occur not only among protons but also among protons and heteronuclei. As an example of the versatility of our model to simulate SABRE-relay experiments, we calculate the time-dependence of polarization transferred to a ^{31}P nucleus in the second organometallic complex C_2 as described by Roy and co-workers.[38] The simulated polarization scheme is as follows: in the first stage, the primary SABRE substrate S_a is polarized at a field of 5 mT. Consequently, the field is lowered to a value, which corresponds to strong coupling between ^{31}P and ^{1}H nuclei. Figure 7(b) shows the evolution of polarization at this second field, which is 1 μT. The simulations demonstrate that the transfer of proton hyperpolarization of the SABRE substrate to the ^{31}P nuclei in the second complex reported[38] can be reasonably well reproduced by the developed model. Our simulations furthermore show that while polarization transfer via J-couplings is efficient between protons, the calculations show no transfer of polarization between protons and ^{13}C or ^{31}P nuclei at the polarization field of 5 mT. These results suggest that the spontaneously formed polarization observed in previous studies[43] might originate from cross-relaxation between protons and ^{13}C spins.

V. CONCLUSION AND OUTLOOK

To summarize, in this work, we present the first theoretical model to describe the emerging hyperpolarization method SABRE-relay. A detailed analysis of the SABRE-relay efficiency on both the spin degrees of freedom (J-couplings and NMR frequencies) as well as on the concentrations and exchange rates of the chemical constituents of this system was conducted in order to guide future development of this field. As SABRE-relay has been shown to be applicable to a stunning number of systems, we do not aim to provide a full description of all possible formulations and applications of the presented theoretical approach but rather aim to lay the groundwork for future developments.

We would also like to outline the main steps of the theory. First, the kinetic scheme should be solved in order to deduce the steady-state concentrations of all species of interest (substrates and complexes). After that, the kinetic equations should be turned into the equations for the density matrices by adding appropriate spin Hamiltonians and relaxation superoperators. When considering reactions transforming different species into each other, one should adapt the dimensionality of their density matrices by using the direct product and partial trace operations. The degree of complexity of the kinetic equations (for the species concentrations and for the corresponding density matrices) depends on in what detail the reaction scheme is treated (one can consider, for instance, multiple-site exchange and additional intermediate complexes). When needed, one can also extend the spin system: adding more spins into consideration is straightforward from a general theoretical perspective but might be computationally very demanding. The degree of complexity required to treat real systems will become clear when comparing the theory to a comprehensive set of experimental data. To ease such comparison, it might become necessary to supply the theory with relevant parameters determined from independent measurements (e.g., NMR analysis of SABRE complexes and measurements of relevant exchange rates).

By using the proposed method, one can analyze the dependence of polarization on kinetic and spin parameters of the system under consideration, which is the crucial step for understanding the efficiency of the SABRE-relay approach and for optimizing its performance. We anticipate that the present treatment can support the development of SABRE-relay and its extension to a broad range of substrates, which cannot be polarized by the traditional SABRE method.

ACKNOWLEDGMENTS

K.L.I. acknowledges support from the Russian Science Foundation (Project No. 19-43-04116), and G.B. acknowledges financial support from the Deutsche Forschungsgemeinschaft under Contract No. Bu-911-29-1.

APPENDIX A: TIME DEPENDENCE OF POLARIZATION

In this appendix, we provide exemplary time traces for the numerical integration of the two different SABRE relay approaches described above.

The representative time traces for both SABRE-relay mechanisms are shown in Figs. 8 and 9. In both cases, the behavior of polarization is qualitatively the same: primarily S_a is polarized in the first SABRE complex. At later times, polarization is transferred to S_b either by chemical exchange or by polarization transfer in the second complex. Polarization of S_b is thus build-up at later times and to a lower level. In the analysis presented in the main part of this paper, we present only the steady-state solutions for polarization, achieved at $t \to \infty$.

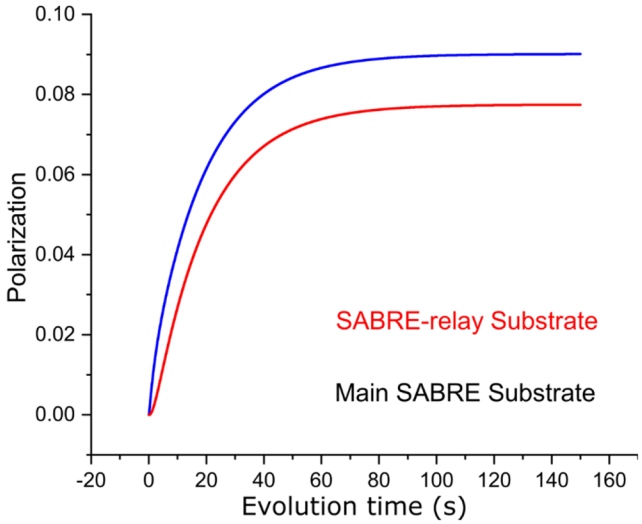

FIG. 8. Temporal evolution of polarization of the proton of the main SABRE substrate (S_a, blue) and the SABRE-relay substrate (S_b, red). Here, T_1 of both substrates was 30 s, and the J-coupling connecting them was assumed to be 10 Hz.

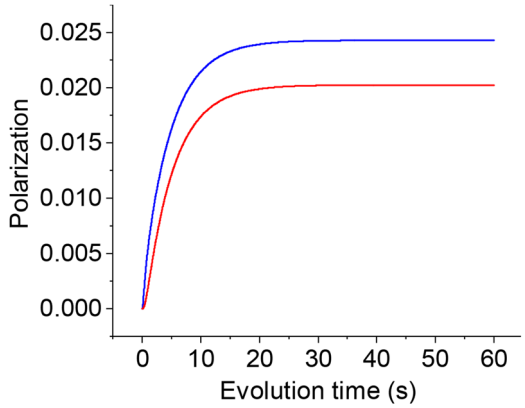

FIG. 9. Temporal evolution of polarization of the proton of the main SABRE substrate (S_{1a}, blue) and the SABRE-relay substrate (S_b, red). Here, the chemical exchange rate k_{ab} was 1 s.

APPENDIX B: DETAILS OF THE SIMULATION

In the following, we briefly reiterate the density matrix treatment used to calculate the effects of exchange here. This approach has been described in detail previously, and we refer the interested reader to the appropriate literature.[46] Let us again assume that we are dealing with two species A and B with concentrations [A] and [B] whose spin system is described by two normalized density matrices $\hat{\rho}_A$ and $\hat{\rho}_B$. First, we choose to normalize all density matrices by their concentrations,

$$\hat{\sigma}_A = \hat{\rho}_A[A], \quad \hat{\sigma}_B = \hat{\rho}_B[B]. \tag{B1}$$

Under such normalization, the trace of each density matrix is proportional to the corresponding concentration. If we assume that these two species coordinate to form a complex,

$$A + B \leftrightarrow C, \tag{B2}$$

we need to introduce appropriate terms in the equations for the density matrices. When the spins of A and B are coupled in the complex C, they should be described by a common density matrix $\hat{\sigma}_C$. If this reaction proceeds with a rate constant k^a, then association contributes to the differential equation governing the dynamics of $\hat{\sigma}_C$ in the following way:

$$\left\{\frac{d}{dt}\hat{\sigma}_C\right\}_{ass} = k^a\{\hat{\sigma}_A \otimes \hat{\sigma}_B\}. \tag{B3}$$

If the complex C dissociates again into its components A and B, we treat this by assuming (justified by the random nature of exchange in a large ensemble)[50] that all coherences between A and B, which may have existed in the complex, are lost. Thus, such a dissociation process, governed by a dissociation rate k_d, contributes to the differential equations of $\hat{\sigma}_A$ and $\hat{\sigma}_B$ in the following way:

$$\left\{\frac{d}{dt}\hat{\sigma}_A\right\}_{diss} = \mathrm{Tr}_B\{\hat{\sigma}_C\}, \quad \left\{\frac{d}{dt}\hat{\sigma}_B\right\}_{diss} = \mathrm{Tr}_A\{\hat{\sigma}_C\}, \tag{B4}$$

where Tr_X is the partial trace operation over the states of the spin system X.

The parameters of the spin system used in this work, unless stated otherwise, can be found in Table I. Accordingly, the concentrations and exchange rates are summarized in Table II.

TABLE I. Parameters of the spin systems used in calculations, *J*-couplings in the two SABRE complexes, chemical shifts, and relaxation rates ($R = 1/T_1 = 1/T_2$). All nuclei are protons.

		J (Hz)		R_1 (s^{-1})	δ (ppm)
SABRE complex	H_1	H_2	S_a		
H_1		−7.7		1	−22
H_2	−7.7			1	−22
S_a	0	1		0.3	8.3
SABRE-relay complex	S_1	S_2			
S_a		1		1	8.3
S_b	1			1	8.3
Free SABRE substrate					
S_a				0.2	8
SABRE relay substrate					
S_a				0.2	8

TABLE II. Chemical parameters used in calculations.

Species	Concentrations (mM)	Exchange rates (s^{-1})
SABRE complex	1	$k_{ab} = 10$
SABRE-relay complex	1	$k_d = 20$
S_a	30	
S_b	30	

DATA AVAILABILITY

The data that support the findings of this study are available from the corresponding author upon reasonable request.

REFERENCES

[1] R. W. Adams, J. A. Aguilar, K. D. Atkinson, M. J. Cowley, P. I. P. Elliott, S. B. Duckett, G. G. R. Green, I. G. Khazal, J. López-Serrano, and D. C. Williamson, Science **323**, 1708 (2009).
[2] K. D. Atkinson, M. J. Cowley, P. I. P. Elliott, S. B. Duckett, G. G. R. Green, J. López-Serrano, and A. C. Whitwood, J. Am. Chem. Soc. **131**, 13362 (2009).
[3] M. J. Cowley, R. W. Adams, K. D. Atkinson, M. C. R. Cockett, S. B. Duckett, G. G. R. Green, J. A. B. Lohman, R. Kerssebaum, D. Kilgour, and R. E. Mewis, J. Am. Chem. Soc. **133**, 6134 (2011).
[4] M. L. Truong, T. Theis, A. M. Coffey, R. V. Shchepin, K. W. Waddell, F. Shi, B. M. Goodson, W. S. Warren, and E. Y. Chekmenev, J. Phys. Chem. C **119**, 8786 (2015).
[5] A. S. Kiryutin, A. V. Yurkovskaya, H. Zimmermann, H.-M. Vieth, and K. L. Ivanov, Magn. Reson. Chem. **56**, 651 (2018).
[6] Z. Zhou, J. Yu, J. F. P. Colell, R. Laasner, A. Logan, D. A. Barskiy, R. V. Shchepin, E. Y. Chekmenev, V. Blum, W. S. Warren, and T. Theis, J. Phys. Chem. Lett. **8**, 3008 (2017).

[7]T. Theis, M. L. Truong, A. M. Coffey, R. V. Shchepin, K. W. Waddell, F. Shi, B. M. Goodson, W. S. Warren, and E. Y. Chekmenev, J. Am. Chem. Soc. **137**, 1404 (2015).
[8]R. V. Shchepin, L. Jaigirdar, T. Theis, W. S. Warren, B. M. Goodson, and E. Y. Chekmenev, J. Phys. Chem. C **121**, 28425 (2017).
[9]J. F. P. Colell, M. Emondts, A. W. J. Logan, K. Shen, J. Bae, R. V. Shchepin, G. X. Ortiz, P. Spannring, Q. Wang, S. J. Malcolmson, E. Y. Chekmenev, M. C. Feiters, F. P. J. T. Rutjes, B. Blümich, T. Theis, and W. S. Warren, J. Am. Chem. Soc. **139**, 7761 (2017).
[10]A. M. Olaru, T. B. R. Robertson, J. S. Lewis, A. Antony, W. Iali, R. E. Mewis, and S. B. Duckett, ChemistryOpen **7**, 97 (2018).
[11]R. V. Shchepin, B. M. Goodson, T. Theis, W. S. Warren, and E. Y. Chekmenev, ChemPhysChem **18**, 1961 (2017).
[12]M. J. Burns, P. J. Rayner, G. G. R. Green, L. A. R. Highton, R. E. Mewis, and S. B. Duckett, J. Phys. Chem. B **119**, 5020 (2015).
[13]V. V. Zhivonitko, I. V. Skovpin, and I. V. Koptyug, Chem. Commun. **51**, 2506 (2015).
[14]R. E. Mewis, K. D. Atkinson, M. J. Cowley, S. B. Duckett, G. G. R. Green, R. A. Green, L. A. R. Highton, D. Kilgour, L. S. Lloyd, J. A. B. Lohman, and D. C. Williamson, Magn. Reson. Chem. **52**, 358 (2014).
[15]K. V. Kovtunov, B. E. Kidd, O. G. Salnikov, L. B. Bales, M. E. Gemeinhardt, J. Gesiorski, R. V. Shchepin, E. Y. Chekmenev, B. M. Goodson, and I. V. Koptyug, J. Phys. Chem. C **121**, 25994 (2017).
[16]Q. Wang, K. Shen, A. W. J. Logan, J. F. P. Colell, J. Bae, G. X. Ortiz, Jr., T. Theis, W. S. Warren, and S. J. Malcolmson, Angew. Chem., Int. Ed. **56**, 12112 (2017).
[17]M. G. Pravica and D. P. Weitekamp, Chem. Phys. Lett. **145**, 255 (1988).
[18]C. R. Bowers and D. P. Weitekamp, J. Am. Chem. Soc. **109**, 5541 (1987).
[19]C. R. Bowers and D. P. Weitekamp, Phys. Rev. Lett. **57**, 2645 (1986).
[20]T. C. Eisenschmid, R. U. Kirss, P. P. Deutsch, S. I. Hommeltoft, R. Eisenberg, J. Bargon, R. G. Lawler, and A. L. Balch, J. Am. Chem. Soc. **109**, 8089 (1987).
[21]J. B. Hövener, N. Schwaderlapp, T. Lickert, S. B. Duckett, R. E. Mewis, L. A. R. Highton, S. M. Kenny, G. G. R. Green, D. Leibfritz, J. G. Korvink, J. Hennig, and D. von Elverfeldt, Nat. Commun. **4**, 2946 (2013).
[22]A. N. Pravdivtsev, A. V. Yurkovskaya, H.-M. Vieth, and K. L. Ivanov, J. Phys. Chem. B **119**, 13619 (2015).
[23]R. W. Adams, S. B. Duckett, R. A. Green, D. C. Williamson, and G. G. R. Green, J. Chem. Phys. **131**, 194505 (2009).
[24]A. N. Pravdivtsev, K. L. Ivanov, A. V. Yurkovskaya, P. A. Petrov, H.-H. Limbach, R. Kaptein, and H.-M. Vieth, J. Magn. Reson. **261**, 73 (2015).
[25]A. N. Pravdivtsev, A. V. Yurkovskaya, H.-M. Vieth, K. L. Ivanov, and R. Kaptein, ChemPhysChem **14**, 3327 (2013).
[26]D. A. Barskiy, R. V. Shchepin, A. M. Coffey, T. Theis, W. S. Warren, B. M. Goodson, and E. Y. Chekmenev, J. Am. Chem. Soc. **138**, 8080 (2016).
[27]K. V. Kovtunov, L. M. Kovtunova, M. E. Gemeinhardt, A. V. Bukhtiyarov, J. Gesiorski, V. I. Bukhtiyarov, E. Y. Chekmenev, I. V. Koptyug, and B. M. Goodson, Angew. Chem., Int. Ed. **56**, 10433 (2017).
[28]J. F. P. Colell, A. W. J. Logan, Z. Zhou, R. V. Shchepin, D. A. Barskiy, G. X. Ortiz, Q. Wang, S. J. Malcolmson, E. Y. Chekmenev, W. S. Warren, and T. Theis, J. Phys. Chem. C **121**, 6626 (2017).
[29]A. N. Pravdivtsev, A. V. Yurkovskaya, H. Zimmermann, H.-M. Vieth, and K. L. Ivanov, Chem. Phys. Lett. **661**, 77 (2016).
[30]A. N. Pravdivtsev, A. V. Yurkovskaya, H.-M. Vieth, and K. L. Ivanov, Phys. Chem. Chem. Phys. **16**, 24672 (2014).
[31]S. Knecht, A. S. Kiryutin, A. V. Yurkovskaya, and K. L. Ivanov, Mol. Phys. **117**, 2762 (2018).
[32]S. Knecht, A. S. Kiryutin, A. V. Yurkovskaya, and K. L. Ivanov, J. Magn. Reson. **287**, 10 (2018).
[33]K. D. Atkinson, M. J. Cowley, S. B. Duckett, P. I. P. Elliott, G. G. R. Green, J. López-Serrano, I. G. Khazal, and A. C. Whitwood, Inorg. Chem. **48**, 663 (2009).
[34]T. Theis, N. M. Ariyasingha, R. V. Shchepin, J. R. Lindale, W. S. Warren, and E. Y. Chekmenev, J. Phys. Chem. Lett. **9**, 6136 (2018).
[35]T. Theis, M. Truong, A. M. Coffey, E. Y. Chekmenev, and W. S. Warren, J. Magn. Reson. **248**, 23 (2014).
[36]S. S. Roy, G. Stevanato, P. J. Rayner, and S. B. Duckett, J. Magn. Reson. **285**, 55 (2017).
[37]D. A. Barskiy, S. Knecht, A. V. Yurkovskaya, and K. L. Ivanov, Prog. Nucl. Magn. Reson. Spectrosc. **114-115**, 33 (2019).
[38]S. S. Roy, K. M. Appleby, E. J. Fear, and S. B. Duckett, J. Phys. Chem. Lett. **9**, 1112 (2018).
[39]W. Iali, P. J. Rayner, and S. B. Duckett, Sci. Adv. **4**, eaao6250 (2018).
[40]W. Iali, P. J. Rayner, A. Alshehri, A. J. Holmes, A. J. Ruddlesden, and S. B. Duckett, Chem. Sci. **9**, 3677 (2018).
[41]P. J. Rayner, B. J. Tickner, W. Iali, M. Fekete, A. D. Robinson, and S. B. Duckett, Chem. Sci. **10**, 7709 (2019).
[42]P. M. Richardson, R. O. John, A. J. Parrott, P. J. Rayner, W. Iali, A. Nordon, M. E. Halse, and S. B. Duckett, Phys. Chem. Chem. Phys. **20**, 26362 (2018).
[43]P. M. Richardson, W. Iali, S. S. Roy, P. J. Rayner, M. E. Halse, and S. B. Duckett, Chem. Sci. **10**, 10607 (2019).
[44]G. Buntkowsky, J. Bargon, and H.-H. Limbach, J. Am. Chem. Soc. **118**, 8677 (1996).
[45]S. Knecht and K. L. Ivanov, J. Chem. Phys. **150**, 124106 (2019).
[46]S. Knecht, A. N. Pravdivtsev, J.-B. Hövener, A. V. Yurkovskaya, and K. L. Ivanov, RSC Adv. **6**, 24470 (2016).
[47]S. Knecht, A. S. Kiryutin, A. V. Yurkovskaya, and K. L. Ivanov, J. Magn. Reson. **287**, 74 (2018).
[48]E. W. Zhao, R. Maligal-Ganesh, Y. Du, T. Y. Zhao, J. Collins, T. Ma, L. Zhou, T.-W. Goh, W. Y. Huang, and C. R. Bowers, Chem **4**, 1387 (2018).
[49]D. A. Barskiy, A. N. Pravdivtsev, K. L. Ivanov, K. V. Kovtunov, and I. V. Koptyug, Phys. Chem. Chem. Phys. **18**, 89 (2016).
[50]K. L. Ivanov, N. N. Lukzen, A. A. Kipriyanov, and A. B. Doktorov, Phys. Chem. Chem. Phys. **6**, 1706 (2004).
[51]K. L. Ivanov, N. N. Lukzen, and A. B. Doktorov, J. Chem. Phys. **121**, 5115 (2004).
[52]A. N. Pravdivtsev and J.-B. Hövener, Chem.-Eur. J. **25**, 7659 (2019).
[53]S. Lehmkuhl, M. Emondts, L. Schubert, P. Spannring, J. Klankermayer, B. Blümich, and P. P. M. Schleker, ChemPhysChem **18**, 2426 (2017).
[54]M. Emondts, D. Schikowski, J. Klankermayer, and P. P. M. Schleker, ChemPhysChem **19**, 2614 (2018).
[55]K. Ivanov, A. Yurkovskaya, and H.-M. Vieth, J. Chem. Phys. **129**, 234513 (2008).
[56]C. Bengs and M. H. Levitt, J. Magn. Reson. **310**, 106645 (2020).